COMMUNICATION

Humidity- and Photo-Induced Mechanical Actuation of Cross-Linked Liquid Crystal Polymers

*Yuyun Liu, Bo Xu, Shengtong Sun, Jia Wei, Limin Wu, and Yanlei Yu**

In nature, plants have the capability to convert simple environmental stimuli into diverse mechanical motions.[1,2] For example, seedling phototropism is a widely examined phenomena triggered by sunlight, leading to differential translocation of auxin to the shaded side of the coleoptile where a curve forms.[3,4] Except for the well-known phototropism movement, morning glory flowers show shape deformation responsive to humidity as well.[5] The ubiquitous presence of humidity in ambient air and its variation makes the development of humidity-responsive actuators both appealing and of importance.[6–13] Recently, polymer gels, graphene monolayer papers, and electroactive polymers have been widely developed to fabricate various humidity-driven actuators.[14–21] For instance, poly(*N*-isopropylacrylamide)-based films have been reported to act as muscles or arms to lift masses in response to humidity;[6] a polymer film combining polypyrrole was demonstrated to be able to drive a piezoelectric element to convert the mechanical energy into electrical energy by using a water gradient as its energy source;[12] and Naumov and Zhang reported an agarose-based film which exhibited fast locomotion driven by humidity.[14] These humidity-responsive films contain typical hydrophilic groups such as hydroxyl, amide, carboxyl, or pyrrolyl, which are easy to interact with water molecules to induce macroscopic deformation. However, different films in the same set of experiments often do not show any consistency in the direction of bending mainly since it is difficult to guide the orientation of those aforementioned humidity-responsive materials. Naumov and co-workers designed actuators with a bilayer structure and achieved anisotropic mechanical deformation by introducing parallel glass fibers to direct the mechanical reconfiguration of the hygroresponsive agarose.[15] Generally, bilayer actuators suffer from delamination of the two layers after long-term exposure to moisture, resulting in a decreased lifetime.[16] Therefore, straightforwardly engineering molecular alignment in a single layered actuator is a preferable way to achieve macroscopic deformation with a predefined direction.[17,18]

Y. Y. Liu, B. Xu, Dr. J. Wei, Dr. L. M. Wu, Prof. Y. L. Yu
Department of Materials Science and State
Key Laboratory of Molecular Engineering of Polymers
Fudan University
Shanghai 200433, P. R. China
E-mail: ylyu@fudan.edu.cn
Dr. S. T. Sun
School of Chemistry Engineering
State Key Laboratory of Chemical Engineering
East China University of Science and Technology
Shanghai 200237, P. R. China

DOI: 10.1002/adma.201604792

The orientation of liquid crystals (LCs) on the nanometer scale is easily manipulated by using alignment layers and fixed by polymerization.[22,23] Therefore, cross-linked LC polymers (CLCPs) have been chosen as preferred candidates for smart actuators.[24–29] Especially, cooperative motion of molecules in CLCPs is the most prominent advantage in changing the molecular alignment by a small amount of energy such as heat, electricity, and light, which gives rise to a macroscopic deformation with a predefined direction.[30] For instance, azobenzene-containing CLCPs have been widely developed into diverse photoresponsive soft actuators owing to the reversible *trans-cis* isomerization of azobenzene and the following LC alignment change.[31–41] In addition, CLCP actuators which deform as a response to changes in humidity have been prepared by combination with hydrogen-bonded carboxylic acid moieties. These materials can absorb water and swell along the direction perpendicular to the alignment director after converting it to a hygroscopic polymer salt in a basic solution.[13,42–44] It is generally believed that hydrophobic CLCPs have no such responsibility to moisture or humidity. Herein, nevertheless, we demonstrate that a hydrophobic, porosity-free CLCP film without hydrogen-bonded LCs is able to undergo rapid macroscopic deformation in response to a humidity gradient. By means of hydration of the C=O and C—O—C groups in the LCs, the film surface swells and the alignment of mesogens changes causing the bending of the whole film along the direction perpendicular to the alignment direction. In addition, owing to containing the azobenzene chromophores, the CLCP film performs interesting dual-responsive actuations stimulated by both humidity and light in predefined ways inspired by both the phototropic growth movements of a seedling and the humidity-responsive blooming of morning glory flowers to convert diverse environmental energy into mechanical actuation effectively.

The CLCP films were prepared by photopolymerization of a LC mixture of a monomer (A11AB6) containing an azobenzene moiety and a diacrylate cross-linker (C3A) with a molar ratio of 60/40 in the presence of 2 mol% of a photoinitiator in a glass cell coated with rubbed polyimide alignment layers (**Figure 1**a and Section S1, Supporting Information). The planar alignment of the film was confirmed with crossed polarizers (Figure S1, Supporting Information). The thickness of the CLCP films was controlled by changing the spacing of glass cells and the films with a typical thickness of 14 μm confirmed by a super-resolution digital microscope were used in most of our studies unless otherwise stated.

We prepared a "tree" from a CLCP film, the deflection of which was induced toward the non-exposed side when a human finger approached it but without direct contact (Figure 1b).

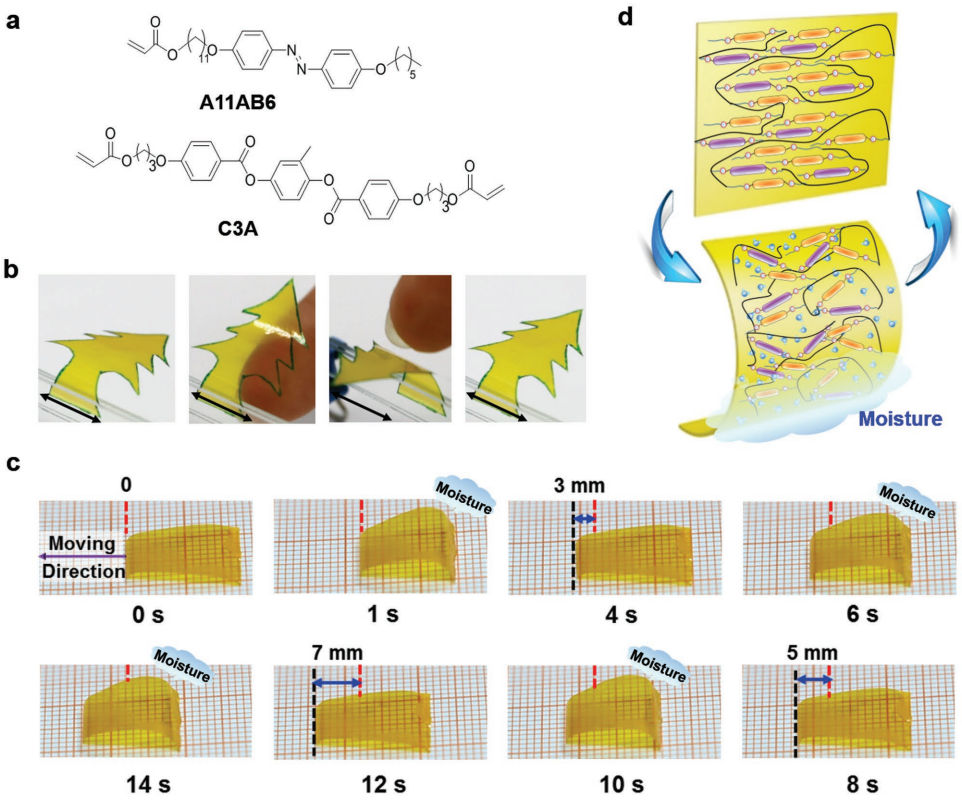

Figure 1. a) Chemical structures of the liquid crystal monomer A11AB6 and cross-linker C3A used for preparation of the CLCP film. b) Photographs showing the "tree" bending. When a finger is close to the back of "tree," it bends in the direction perpendicular to the LC alignment direction and changes from a backbends to a forward bends, while it recovers to its original state after the finger is removed. The double-headed arrows represent the mesogens alignment direction. c) Time course of the walking motion of the CLCP film with different end shapes (Length = 17 mm; $Width_{left}$ = 8 mm; $Width_{right}$ = 11 mm). Upon exposure to the moisture from the upper right side of the film, the right edge retracts inward and the film extends to the left side after removing the moisture. The red dashed lines represent the starting line; the black dashed lines represent the left edge of the film. d) Schematic representation of the humidity-responsive principle of the bending of the actuators. When moisture approaches to one side of the monodomain CLCP film, the alignment of mesogens changes and the surface undergoes anisotropic swelling, resulting in the bending of the CLCP film along the direction perpendicular to the LCs alignment direction.

When the finger approached the back of "tree," it spontaneously started to bend perpendicular to the LC alignment direction to overcome the gravity and changed from backbends to forward bends in a few seconds (Movie S1, Supporting Information). It clearly demonstrates that even a slight and local humidity increase close to the CLCP film readily induces fast bending; that is, the CLCP film exhibits high sensitivity to the presence of uncovered human skin. Furthermore, "tree" recovered its original state in 10 s after removing the finger, indicating that the bending was completely reversible. When we put the monodomain CLCP film on a hand which is on the top of a steel plate with an earthing wire to remove the static electricity, the film exhibited obvious deformation immediately, proving that the humidity gradients induce the bending of the monodomain CLCP film rather than static electricity (Figure S2a and Movie S2, Supporting Information). However, when we put a piece of the CLCP film on a hand in a rubber glove, the film did not bend, proving that the bending behavior is not driven by a temperature gradient (Figure S2b, Supporting Information).

The CLCP film with excellent humidity-responsive properties was further designed to demonstrate a worm-like motion stimulated by humidity gradients (Movie S3, Supporting Information). Figure 1c shows the successive profiles of the unidirectional motion of the CLCP film (Length = 17 mm; $Width_{left}$ = 8 mm; $Width_{right}$ = 11 mm) with different end shapes induced by humidity gradients. At the beginning of each actuation cycle, we used nitrogen gas flow to transport moisture to the right upside of the film (Section S2, Supporting Information), causing the right part of the film to bend inward. After removing the moisture, the right edge bearing larger frictional force acts as a stationary point and thus the unbending of the film leads the left part to move outward and the whole film to extend toward the left direction. As Movie S3 (Supporting Information) shows, the moving speed of the CLCP "worm" is about 45 mm min^{-1}.

It is interesting to note that the CLCP film spontaneously flipped and moved swiftly across the substrate in succession once placed on a 40 °C moist fabric substrate (Movie S4, Supporting Information). When the CLCP film contacts the moist substrate, the bottom surface absorbs more moisture than the top surface and the film underdoes an asymmetric swell along the thickness direction and finally rolls up. Subsequently, the gravity center of the film rises and becomes unstable, which eventually causes the curved film to topple over. In contrast

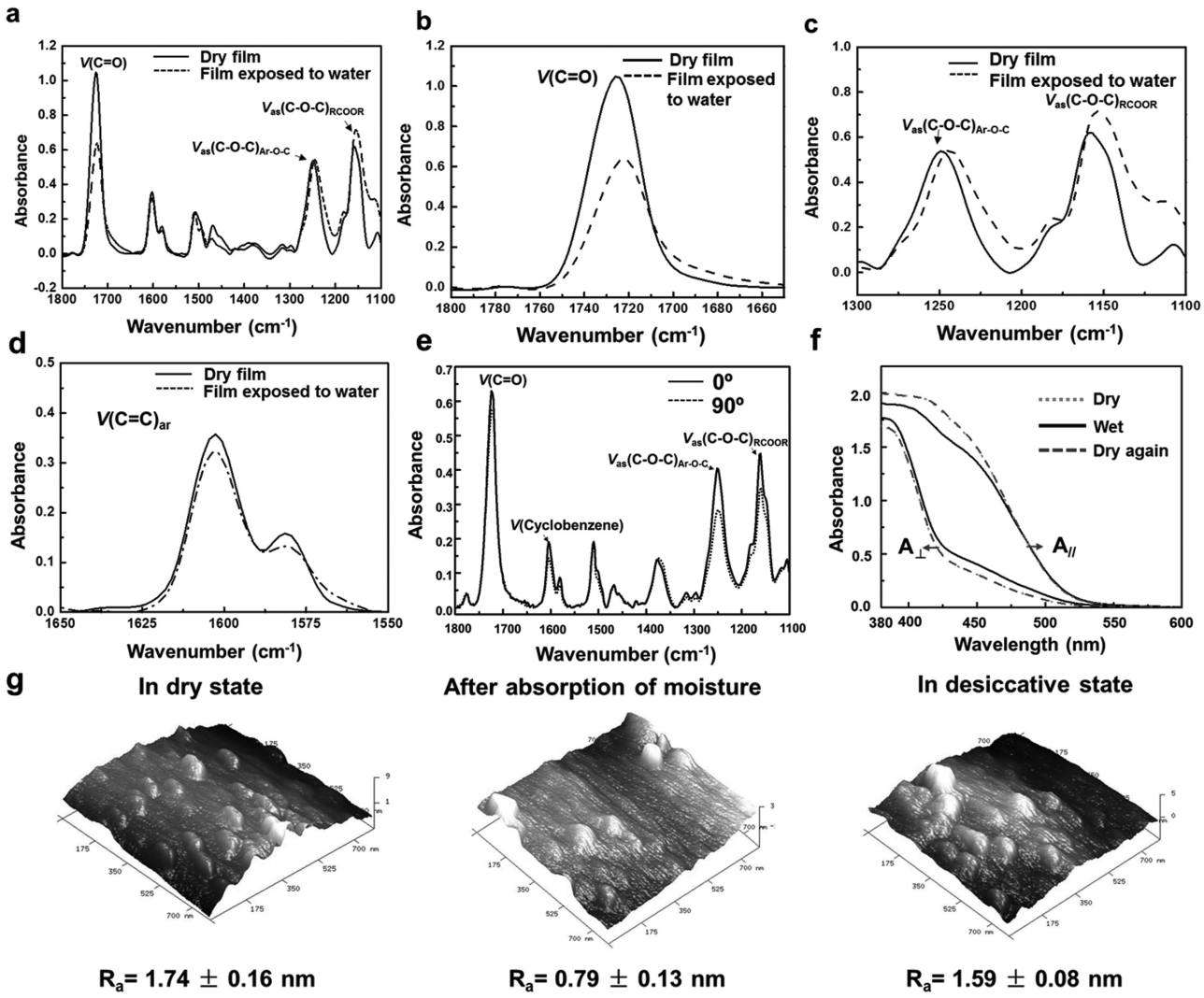

Figure 2. ATR-FTIR spectra of the CLCP film before (solid line) and after absorption of moisture (dashed line) in the region of a) 1800–1000 cm^{-1}, b) C=O stretching band (ν(C=O)), c) C—O—C stretching bands (ν(C—O—C)), and d) skeleton vibrational band of aromatic ring (ν(C=C)$_{ar}$). e) Polarized ATR-FTIR spectra of the CLCP film at room temperature with the polarized IR beam parallel (solid line) or perpendicular (dashed line) to the rubbing direction. f) Polarized UV–vis absorption spectra of the CLCP film. $A_{//}$ and $A_{\perp}$ are the absorbance measured with polarized light parallel and perpendicular to the rubbing direction of the alignment layers, respectively. $A_{//}$ in the dry state is much higher than $A_{\perp}$; after the film is immersed in water for 30 min, $A_{\perp}$ increases and $A_{//}$ decreases; when the film is dry again, both $A_{//}$ and $A_{\perp}$ recover to the initial state. Thickness of the film: 5 μm. g) In situ AFM height images of the monodomain CLCP film in dry state, after moisture absorption and desorption, respectively. The surface average roughness is 1.74 ± 0.16, 0.79 ± 0.13, and 1.59 ± 0.08 nm, respectively. The scanning size: 800 × 800 nm.

to previous humidity-responsive films whose bending directions had no consistency during the flipping process, such as a polypyrrole/polyol-borate film,[12] a graphene monolayer film,[45] and an agarose-based film,[46] the bending direction of the CLCP film on a moist substrate was always perpendicular to the mesogens alignment direction.

In general, humidity-responsive materials contain typical hydrophilic groups, which are easy to interact with water molecules to induce macroscopic deformation. The CLCP films, however, have a hydrophobic nature with a water contact angle of 91.5° (Figure S3, Supporting Information) demonstrating incredible humidity-responsive behavior. Attenuated total reflectance Fourier transform infrared (ATR-FTIR) spectra of the film before and after immersing into deionized water for 10 min were measured to elucidate the internal changes at the molecular level (**Figure 2**a–d). The regions in response to the C=O and C—O—C stretching bands shift to lower wavenumbers by ≈4 cm^{-1} after water diffuses into the film (Figure 2b,c), while the skeleton vibrational band of aromatic rings (ν(C=C)$_{ar}$) shows no obvious shift (Figure 2d), suggesting the hydration of hydrophobic ester linkages and the formation of hydrogen bonds between ether oxygen groups and water molecules.[47–49] This hydrogen bonding interaction between CLCP and water molecules leads the CLCP film to absorb moisture from the humid air.

The polarized ATR-FTIR spectra of the CLCP films were also collected at room temperature (Figure 2e). It is noted that when the polarization direction of IR beam is parallel to the

rubbing direction, the absorbance of aromatic rings and oxygen-containing groups reaches a maximum value; when the two directions are perpendicular to each other, the absorbance of these groups is at a minimum value. This clearly demonstrates that the azobenzene moieties and oxygen-containing groups are preferentially aligned along the rubbing direction of the alignment layers.

We further investigated whether the CLCP film undergoes the order degree change of mesogens after the absorption of moisture by measuring the polarized UV–vis absorption spectra of the film in both dry and wet states. It is known that azobenzene molecules show angle-dependent absorption of linearly polarization light.[50,51] Order parameter (S) of the film in different conditions was evaluated by the following equation:

$$S = (A_{//} - A_{\perp})/(A_{//} + 2A_{\perp}) \quad (1)$$

where $A_{//}$ and $A_{\perp}$ are the absorbance measured with light polarized parallel and perpendicular to the rubbing direction of the alignment layers, respectively (Table S1, Supporting Information). As shown in Figure 2f, $A_{//}$ of the film in dry condition was higher than $A_{\perp}$ and the order parameter was calculated to be 0.14. After the film was immersed in water for 30 min to enable the oxygen-containing groups to completely form hydrogen bonds with water molecules in the CLCP film, the difference between $A_{//}$ and $A_{\perp}$ decreased, resulting in the descent of the order parameter to be 0.09. When the film was dried again, the value of S returned to 0.14. These results demonstrate that azobenzene mesogens in the dry film are preferentially aligned along the rubbing direction of the alignment layer, while the alignment of mesogens in the humid film decreases due to the hydrogen bonding interaction between CLCP and water molecules.

As shown in Figure 1d, when one side of the CLCP film is exposed to moisture, the LCs have interaction with water molecules causing the swelling of this side and the film bending away from the moisture. Furthermore, the hydrogen bonding interaction leads to the decrease of mesogens order degree, which results in the expansion perpendicular to the alignment direction. Considering all these factors, the swelling of the film surface mainly takes place in the direction perpendicular to the alignment direction on this surface. Thus, the whole CLCP film undergoes a fast bending along the direction perpendicular to the LC alignment direction. To investigate the role of the mesogens orientation in the humidity-responsive deformation of the film, we also prepared a polydomain CLCP film by in situ photopolymerization at 105 °C (in an isotropic phase of the LC mixture) in a glass cell coated with polyimide alignment layers without rubbing treatment (Section S1, Supporting Information). The polydomain CLCP film had a slight deformation in an uncertain direction when placed on a 40 °C moisture fabric substrate due to the isotropic swell of the film (Figure S4, Supporting Information), since the film consisted of many micro-sized domains of mesogens aligned in one direction in each domain, but macroscopically the direction of alignment was random. The polarized UV–vis absorption spectra of the polydomain CLCP film in both dry and wet states were also measured. As Figure S5 (Supporting Information) shows, the absorbance has no obvious change after the polydomain CLCP film absorbs moisture. These results also manifest that the bending behavior of the monodomain CLCP film is closely related to the parallel alignment of the mesogens, which brings about the anisotropic swell of the film surface and the macroscopic deformation of the film in response to a humidity gradient.

In addition, the surface profile variations of the CLCP films before and after moisture absorption were measured and recorded by atomic force microscopy (AFM). As shown in Figure 2g, the mean roughness (R_a) of the CLCP film in dry conditions with low relative humidity (RH) of ≈20% is 1.74 ± 0.16 nm, while R_a decreases by 55% to be 0.79 ± 0.13 nm when RH increases to ≈55%. In other words, the film surface in wet condition exhibits a more flattened morphology resulted from the penetration of the water molecules and the swell of the whole film, which also indicates the existence of the hydrogen bonding interaction between the LCs and the water molecules. Furthermore, the removal of moisture leads to shrinkage of the film surface, giving rise to the recovery of R_a from 0.79 ± 0.13 to 1.59 ± 0.08 nm and thus more fluctuant creases and irregular wrinkles. The change of the film surface morphology with the RH variation was also proved by confocal microscopy images. It was found that the wrinkles on the film surface faded away at higher RH of ≈55% and R_a decreased by 54% from 3.14 ± 0.2 to 1.46 ± 0.1 nm, while the surface exhibited more fluctuations and R_a increased to 3.17 ± 0.1 nm after the moisture was removed (Figure S6, Supporting Information). The variation of the surface morphology with RH change is ascribed to the absorption and desorption of water molecules to form and disrupt hydrogen bonds in the film, respectively. We further measured the surface profile variation of the polydomain CLCP film before and after moisture absorption by AFM (Figure S7, Supporting Information). No obvious R_a change of the film surface was observed since the isotropic swell of the film was incapable of generating apparent variation in the surface morphology.

To investigate the universality of the humidity-responsive actuation of the CLCP films based on polyacrylates, a 14 μm CLCP film without azobenzene moieties was prepared (Section S1 and Figure S8a, Supporting Information). When exposed to the humidity gradient, it also deformed rapidly along the direction perpendicular to the mesogens alignment direction. Figure S8b (Supporting Information) shows time dependence of the bending curvature change of 14 μm CLCP film without azobenzene moieties upon exposure to 80% RH difference. It reached 1.6 cm^{-1} in 1 s.

The effects of film thickness and RH difference on the bending curvature and speed were quantitatively measured to clearly show how to control the actuation. We employed a humidity chamber with a small hole to adjust the internal RH from ≈30 to ≈90%, while the external RH was kept at ≈10% (**Figure 3**a). The curvature k (cm^{-1}) was calculated as described in Figure S9 (Supporting Information). In addition, we used the same conditions for the experiments to eliminate the effect of a convection flow (Figure S10 and Movie S5, Supporting Information). Figure 3b shows the bending kinetics of CLCP films with different thicknesses upon exposure to the certain RH difference of 80%. Though composed of hydrophobic materials, the CLCP films show fast response to a humidity gradient. For example, the bending speed of the film with the thickness of 14 μm is about 5.8 cm^{-1} s^{-1}, whose curvature at the steady state

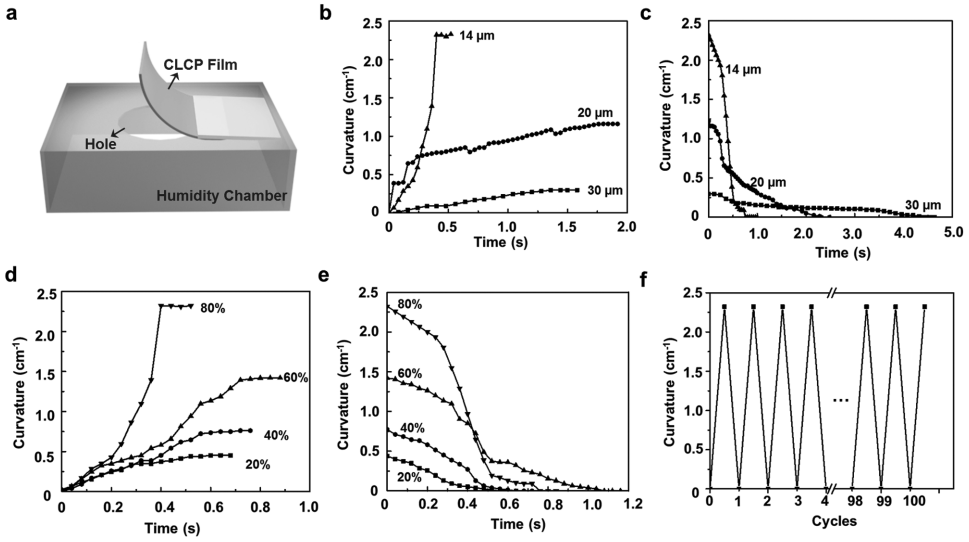

Figure 3. a) Schematic diagram of the homemade humidity chamber used for quantitative measurement of the film deformation curvature. b,c) Plots showing time dependence of the bending curvature change of CLCP films with different thickness upon exposure to 80% RH difference and relaxation dynamics after removing the humidity exposure. d,e) Plots showing time dependence of the bending curvature for the 14 μm CLCP film upon exposure to different humidity differences and relaxation dynamics after removing the humidity exposure. f) A plot showing the reversible deformation of the 14 μm film upon cyclic exposure to a 80% RH difference. The humidity-induced motion repeats as many as 100 cycles without obvious fatigue.

is 2.3 cm^{-1}. In view of the actuation mechanism, we argue that only a thin hydrated surface layer is formed to drive the bending of the whole film after exposure to the moisture gradient. Therefore, the bending speed and curvature of the film significantly depends on the film thickness. The thinner the film, the faster the bending and the larger the curvature. Figure 3c shows all of the films change back to the flat state quickly in a few seconds when the humidity stimulus is removed, since the thin hydrated layer vanishes by exchanging moisture with the ambient air. Figure 3d shows that the steady-state bending curvature of the 14 μm thick film increases gradually from 0.4 to 2.3 cm^{-1} as RH difference increases from 20% to 80%. The relaxation process toward the flat state was quickly completed in 1 s after removing the exposed moisture (Figure 3e) and the deflection-recovery process of the film repeated over 100 times without obvious fatigue (Figure 3f).

In addition, the CLCP film containing the azobenzene chromophores shows UV-induced actuation as well. When irradiated by UV light (365 nm, 40 mW cm^{-2}), the CLCP film bended toward the incidence direction of the UV light along the LCs alignment direction, while recovering to the initial state upon visible light irradiation (530 nm, 60 mW cm^{-2}) (Figure S11, Supporting Information). It is the first time to achieve humidity- and photo-dual-responsive CLCP actuators. Though some humidity-responsive films have shown their actuation in response to both humidity and infrared light, the infrared light functions as a heat source to change RH and induces deformation of films, which restricts their actuation performance.[45] For example, it is difficult to actuate a graphene monolayer film by using infrared light to change RH when the films are in an environment with low RH. In contrast, the UV-induced actuation of CLCP films owes to a change in the molecular orientation triggered by the *trans-cis* photoisomerization in azobenzenes, which does not depend on the RH values.

Moreover, the bending directions induced by light and humidity are orthogonal, which provides more chances for many unique applications. It should be noted that the CLCP film possessing high sensitivity and rapid response to external stimuli can be utilized in smart touchless electronic devices and dual-responsive detectors. We demonstrated a device with a dual-mode actuation assembled by the CLCP film coated with conductive materials and two light-emitting diode (LED) lights with different colors (**Figure 4**a). Figure 4b shows a circuit diagram of the experimental setup containing two circuits (circuit 1 and 2) which are stimulated by the humidity gradient and UV light, respectively. The initial states of both electrical circuits were open, and then the film bent along the direction vertical to the LC alignment direction by an approaching finger without direct contact, which resulted in the closing of circuit 1 and the illumination of the yellow LED. After the removal of the finger, circuit 1 opened and the yellow LED turned off. When the front side of the film was irradiated with UV light (365 nm, 40 mW cm^{-2}), circuit 2 containing a red LED was closed because the azobenzene moieties on the outmost surface of the film underwent *trans-cis* photoisomerization leading to the bending of the film along the LC alignment direction (Figure 4b,c). After exposure to visible light (530 nm, 60 mW cm^{-2}), the film recovered to a flat state and the red LED turned off (Movie S6, Supporting Information). The CLCP film acted as a dual-responsive single-pole double throw switch.

In summary, we successfully fabricated a hydrophobic CLCP film featuring dual-responsive actuation by utilizing humidity gradients and UV light. By means of the hydration of oxygen-containing groups and LCs alignment, the CLCP film undergoes a fast reversible actuation in a predefined way, that is, perpendicular to the direction of LCs alignment, by exposure to humidity gradients, which is superior to other state-of-the-art materials. The CLCP film also performed a series of

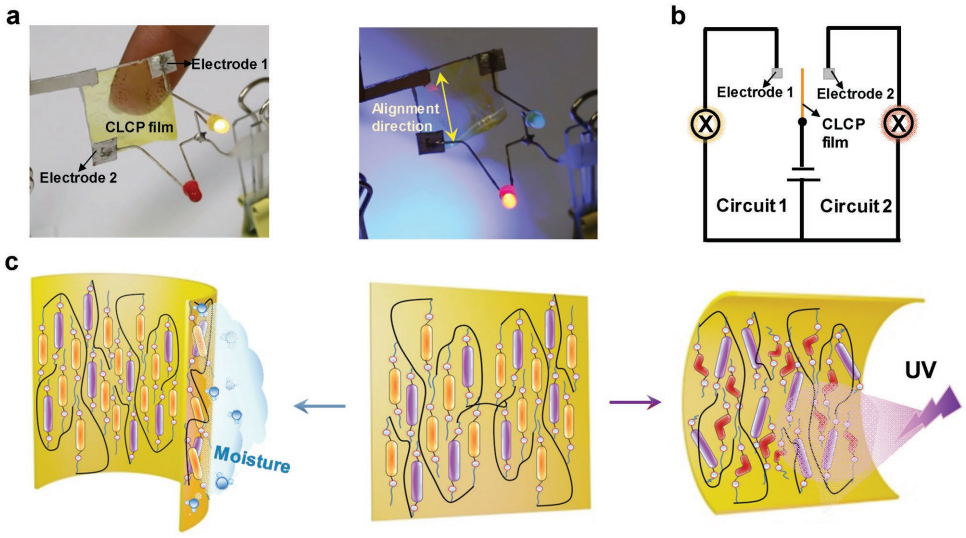

Figure 4. a) Photographs of the CLCP film as a dual-mode sensor which was assembled by a CLCP film coated with conductive materials and two LED lights of different colors. The top edge and left edge of the CLCP film are covered with silver ink. The double arrow represents the alignment direction of the CLCP film. When a finger approaches the back of the CLCP film, the film bends along the direction perpendicular to the LC alignment direction, resulting in the closure of circuit 1 and illumination of the yellow LED. When irradiated with UV light toward the front side of the film, the film bends along the LC alignment direction and circuit 2 containing the red LED closes. The intensity of UV light: 40 mW cm^{-2}. b) Parallel circuits diagram of the experimental setup. The gray squares represent electrode 1 and 2. c) Schematic representation of the humidity- and photo-responsive deformation principle of CLCPs. When moisture approaches the back of the CLCP film, the alignment of mesogens changes and the surface undergoes anisotropic swelling, resulting in the bending of the CLCP film along the direction perpendicular to the mesogens alignment direction. Owing to a change in the molecular orientation triggered by the *trans-cis* photoisomerization in azobenzenes, the CLCP film bends upon exposure to UV light.

sophisticated contactless motions by exposure to humidity gradients, including an inchworm walk, a sit-up motion by "tree", and tumbling locomotions. In addition, the CLCP film also exhibited UV-responsive bending along the LCs alignment direction, which is orthogonal to the direction of the bending induced by humidity. Therefore, a touchless electronic device with dual-mode actuation was prepared to output different signals in response to humidity and UV light. This work not only provides new insights into the mechanism of humidity-responsive actuation of hydrophobic CLCP films but also broadens the potential applications of the dual-responsive CLCP films in electronic devices and sensors.

Supporting Information

Supporting Information is available from the Wiley Online Library or from the author.

Acknowledgements

This work was supported financially by the National Natural Science Foundation of China (51225304, 21134003, 21273048, and 51573029), the National Key Research and Development Program (2016YFA0202900), and Shanghai Outstanding Academic Leader Program (No. 15XD1500600).

Received: September 6, 2016
Revised: October 29, 2016
Published online: December 23, 2016

[1] C. Dawson, J. F. V. Vincent, A.-M. Rocca, *Nature* **1997**, *390*, 668.
[2] S. Armon, E. Efrati, R. Kupferman, E. Sharon, *Science* **2011**, *333*, 1726.
[3] M. P. M. Dicker, J. M. Rossiter, I. P. Bond, P. M. Weaver, *Bioinspiration Biomimetics* **2014**, *9*, 36015.
[4] R. A. Sherry, C. Galen, *Plant Cell Environ.* **1998**, *21*, 983.
[5] Y. Ma, J. Q. Sun, *Chem. Mater.* **2009**, *21*, 898.
[6] M. R. Islam, X. Li, K. Smyth, M. J. Serpe, *Angew. Chem. Int. Ed.* **2013**, *52*, 10330.
[7] S. Taccola, F. Greco, E. Sinibaldi, A. Mondini, B. Mazzolai, V. Mattoli, *Adv. Mater.* **2015**, *27*, 1668.
[8] M. Wang, X. L. Tian, R. H. A. Ras, O. Ikkala, *Adv. Mater. Interfaces* **2015**, *2*, 1500080.
[9] Q. Zhao, J. Heyda, J. Dzubiella, K. Täuber, J. W. C. Dunlop, J. Y. Yuan, *Adv. Mater.* **2015**, *27*, 2913.
[10] Y. Geng, P. L. Almeida, S. N. Fernandes, C. Cheng, P. P. Muhoray, M. H. Godinho, *Sci. Rep.* **2013**, *3*, 1028.
[11] X. Chen, L. Mahadevan, A. Driks, O. Sahin, *Nat. Nanotechnol.* **2014**, *9*, 137.
[12] M. M. Ma, L. Guo, D. G. Anderson, R. Langer, *Science* **2013**, *339*, 186.
[13] L. T. de Haan, J. M. N. Verjans, D. J. Broer, C. W. M. Bastiaansen, A. P. H. J. Schenning, *J. Am. Chem. Soc.* **2014**, *136*, 10585.
[14] L. D. Zhang, P. Naumov, *Angew. Chem. Int. Ed.* **2015**, *54*, 1482.
[15] L. D. Zhang, S. Chizhik, Y. Z. Wen, P. Naumov, *Adv. Funct. Mater.* **2016**, *26*, 1040.
[16] T. Kamal, S. Y. Park, *Chem. Commun.* **2014**, *50*, 2030.
[17] H. H. Cheng, J. Liu, Y. Zhao, C. G. Hu, Z. P. Zhang, N. Chen, L. Jiang, L. T. Qu, *Angew. Chem. Int. Ed.* **2013**, *52*, 10482.
[18] S. S. He, P. N. Chen, L. B. Qiu, B. J. Wang, X. M. Sun, Y. F. Xu, H. S. Peng, *Angew. Chem. Int. Ed.* **2015**, *54*, 14880.

[19] P. N. Chen, Y. F. Xu, S. S. He, X. M. Sun, S. W. Pan, J. Deng, D. Y. Chen, H. S. Peng, *Nat. Nanotechnol.* **2015**, *10*, 1077.
[20] H. Okuzaki, T. Kuwabara, K. Funasaka, T. Saido, *Adv. Funct. Mater.* **2013**, *23*, 4400.
[21] L. Liu, S. H. Jiang, Y. Sun, S. Agarwal, *Adv. Funct. Mater.* **2016**, *26*, 1021.
[22] T. Ware, M. M. Conney, J. Wie, V. Tondiglia, T. J. White, *Science* **2015**, *347*, 982.
[23] J. Lv, Y. Y. Liu, J. Wei, E. Q. Chen, L. Qin, Y. L. Yu, *Nature* **2016**, *537*, 179.
[24] T. J. White, D. J. Broer, *Nat. Mater.* **2015**, *14*, 1087.
[25] L. Liu, S. H. Jiang, Y. Sun, S. Agarwal, *Adv. Funct. Mater.* **2016**, *26*, 1021.
[26] J. Wei, Y. L. Yu, *Soft Matter* **2012**, *8*, 8050.
[27] E. K. Fleischmann, R. Zentel, *Angew. Chem. Int. Ed.* **2013**, *52*, 8810.
[28] Z. L. Wu, A. Buguin, H. Yang, J. Taulemesse, N. Moigne, A. Bergeret, X. G. Wang, P. Keller, *Adv. Funct. Mater.* **2013**, *23*, 3070.
[29] M. Warner, E. M. Terentjev, *Liquid Crystal Elastomers*, Oxford University Press, Oxford, UK **2003**.
[30] Y. L. Yu, T. Ikeda, in *Smart Light-Responsive Materials* (Eds: Y. Zhao, T. Ikeda, John Wiley and Sons, Hoboken, NJ **2009**, Ch. 3.
[31] F. T. Cheng, R. Y. Yin, Y. Y. Zhang, C. C. Yen, Y. L. Yu, *Soft Matter* **2010**, *6*, 3447.
[32] H. Finkelmann, E. Nishikawa, G. G. Pereira, M. Warner, *Phys. Rev. Lett.* **2001**, *87*, 015501.
[33] W. Wang, X. Z. Wang, F. T. Cheng, Y. L. Yu, Y. T. Zhu, *Prog. Chem.* **2011**, *23*, 1165.
[34] W. Wang, X. M. Sun, W. Wu, H. S. Peng, Y. L. Yu, *Angew. Chem. Int. Ed.* **2012**, *51*, 4644.
[35] W. Wu, L. M. Yao, T. S. Yang, R. Y. Yin, F. Y. Li, Y. L. Yu, *J. Am. Chem. Soc.* **2011**, *133*, 15810.
[36] Z. Jiang, M. Xu, F. Y. Li, Y. L. Yu, *J. Am. Chem. Soc.* **2013**, *135*, 16446.
[37] C. L. van Oosten, C. W. M. Bastiaansen, D. J. Broer, *Nat. Mater.* **2009**, *8*, 677.
[38] S. Iamsaard, S. J. Asshoff, B. Matt, T. Kudernac, J. J. L. M. Cornelissen, S. P. Fletcher, N. Katsonis, *Nat. Chem.* **2014**, *6*, 229.
[39] D. Q. Liu, D. J. Broer, *Angew. Chem. Int. Ed.* **2014**, *53*, 4542.
[40] S. Serak, N. Tabiryan, R. Vergara, T. J. White, R. A. Vaia, T. J. Bunning, *Soft Matter* **2010**, *6*, 779.
[41] Y. L. Yu, M. Nakano, T. Ikeda, *Nature* **2003**, *425*, 145.
[42] D. J. Broer, C. M. W. Bastiaansen, M. G. Debije, A. P. H. J. Schenning, *Angew. Chem. Int. Ed.* **2012**, *51*, 7102.
[43] K. D. Harris, C. W. M. Bastiaansen, J. Lub, D. J. Broer, *Nano Lett.* **2005**, *5*, 1857.
[44] L. T. de Haan, V. Gimenez-Pinto, A. Konya, T. Nguyen, J. M. N. Verjans, C. Sánchez-Somolinos, J. V. Selinger, R. L. B. Selinger, D. J. Broer, A. P. H. J. Schenning, *Adv. Funct. Mater.* **2014**, *24*, 1251.
[45] J. K. Mu, C. Y. Hou, B. J. Zhu, H. Z. Wang, Y. G. Li, Q. H. Zhang, *Sci. Rep.* **2014**, *5*, 9503.
[46] L. D. Zhang, H. R. Liang, J. Jacob, P. Naumov, *Nat. Commun.* **2015**, *6*, 7862.
[47] Y. L. Su, J. Wang, H. Z. Liu, *Macromolecules* **2002**, *35*, 6426.
[48] S. T. Sun, P. Y. Wu, *Macromolecules* **2013**, *46*, 236.
[49] S. Meng, B. J. Sun, Z. Guo, W. Zhong, Q. G. Du, P. Y. Wu, *Polymer* **2008**, *49*, 2738.
[50] F. T. Cheng, Y. Y. Zhang, R. Y. Yin, Y. L. Yu, *J. Mater. Chem.* **2010**, *20*, 4888.
[51] Y. L. Yu, M. Nakano, A. Shishido, T. Shiono, T. Ikeda, *Chem. Mater.* **2004**, *16*, 1637.